

# Mechanical properties of laminated CuAl10Fe3Mn2 aluminum bronze – intermetallics composites

**M Konieczny**

Kielce University of Technology, Department of Metals Science and Materials Technologies, Poland

E-mail: mkon@tu.kielce.pl

**Abstract.** CuAl10Fe3Mn2-intermetallic phases laminated composites have been fabricated through reactive bonding at 875°C in vacuum using bronze foils (0.3 mm thick) and Ti foils with different initial thickness (0.05, 0.1 and 0.15 mm). The titanium layers were completely consumed during reaction resulting in microstructure of well-bonded bronze-intermetallics composites. The mechanical properties and fracture behavior of the fabricated composites were examined under different loading conditions through tension and impact tests. The results of investigations indicated that tensile properties of the composites strongly depended on the proportion between thickness of individual bronze layers and the thickness of intermetallics. The impact tests showed that when the load was applied perpendicular to the laminates, the composites displayed superior impact toughness. The toughness increased with increasing of remaining bronze thickness. The failure during impact testing occurred by cleavage mode for the specimens loaded parallel to the laminated composites and showed extensive plastic deformation for specimens loaded perpendicularly.

## 1 Introduction

Since almost three decades there has been great interest in the investigation of mechanical behavior of a variety of laminated metal composites, especially from metal-metal [1], metal-ceramic [2] and metal-intermetallic [3-13] systems.

Metal-intermetallic laminated (MIL) composites have the potential to perform various functions, such as heat exchange, blast mitigation, ballistic protection, thermal management and vibration damping [5]. MIL composites combine the ductility and high toughness of metals with the higher elastic modulus, higher strength, and lower density of intermetallics. Lamination improves fracture toughness, fatigue behavior, wear, corrosion and damping capacity. It can also provide enhanced formability or ductility for normally brittle intermetallics [1]. There are two groups of commonly used production techniques of MIL composites: deposition or bonding. Sputtering or vapor deposition techniques involve atomic scale transport of the component materials. Such nano-laminated materials are typically fabricated by depositing hundreds of alternate nanoscale layers and they have received significant interest due to their extremely high strength [13]. Unfortunately deposition techniques require sophisticated manufacturing equipment and are very slow. These factors increase the cost of component production and make these composites economically unattractive. Bonding techniques, e.g. diffusion bonding, transient liquid phase bonding and reaction bonding between metal foils have many advantages. They involve relatively simple processing and the size and the number of layers that can be produced are not limited [3]. Moreover, the laminated



structure of the composite allows for variations in the layer thickness and phase volume fractions of the components simply through the selection of initial foils thickness. A great number of laminated composites have been produced using Al and Ni [3, 6, 8], Ti [5, 11, 12], Nb [4] or Fe [7] foils. Previous works also revealed that titanium-intermetallic and copper-intermetallic composites can be produced by reaction that occurs at the interface of Ti and Cu [8-10]. Aluminum bronzes are corrosion-resistant alloys of copper containing from 4 to 15 % aluminum and small amounts of other metals, used to make many machine parts and tools. Alloys containing approximately 10 % aluminum are fabricated by sand casting and gravity diecasting into strong objects, including ship propellers [14]. The laminated composites with aluminum bronze matrix could be considered for structural applications because of their lower density than monolithic bronze. This kind of laminated composites has been investigated by Tsai et al. [15]. In the previous study [16] the reaction synthesis was successfully employed to fabricate laminated composites in vacuum using aluminum bronze and Ti foils. Designing laminated composites to obtain optimal mechanical requires knowledge of the composite failure mechanism. Many investigators [3-6, 17-22] have analyzed the mechanical and fracture properties of metal-intermetallic laminated composites, and proposed several useful models of crack propagation. The aim of this work is to study the mechanical properties of CuAl10Fe3Mn2 aluminum bronze-intermetallics laminated composites under different loading conditions and volume fraction of constituents.

## 2 Experimental procedure

For bronze-intermetallics laminated composites fabrication titanium foils were alternatively stacked between CuAl10Fe3Mn2 foils of 0.3 mm thickness that were produced by hot rolling.

Chemical composition and mechanical properties of used materials are shown in table 1.

**Table 1.** Chemical composition and mechanical properties of foil materials

Material	Chemical composition (at %)	YS (MPa)	UTS (MPa)	Elongation (%)
<b>Ti</b>	99.51 Ti, 0.09 Fe, 0.08 C, 0.07 Al, 0.18 O, 0.05 V, 0.02 N	250	320	24
	83.36 Cu, 2.78 Fe, 10.75 Al, 1.98 Mn, 0.76 Ni, 0.29 Zn, 0.08 Sn	325	580	12
<b>CuAl10Fe3Mn2</b>				

The titanium foil thicknesses were initially selected (0.05, 0.10 and 0.15 mm thick) to completely consume the metal in forming the intermetallic compounds with alternating layers of partially unreacted bronze. Foils were cut into 60 x 10 mm rectangular pieces. Any contamination was removed in a bath of 5 % HF in water. After rinsing in water, foils were stacked into laminates in an alternating sequence. A pressure of 5 MPa was employed at room temperature in a specially constructed vacuum furnace to ensure good contact between foils. Series of attempts allowed to find that a temperature of at least 870 °C was necessary for the start and rapid development of structural processes at the interface between aluminum bronze and titanium. The temperature was increased from 20 to 800°C at a heating rate of 0.25 °C/s. The samples were heated in vacuum of 0.01 Pa at 800 °C for 1h under applied 5 MPa pressure to allow diffusion bonding of the layers. After that the foils were heated to 875°C and held at this temperature for 60 minutes. The pressure was removed during this processing sequence with the purpose of eliminating possible expulsion of liquid phases. The temperature was then decreased slowly (cooling rate of 0.16 °C/s) to 700 °C and the pressure of 5 MPa was applied again. Finally, the samples were furnace-cooled to room temperature (figure 1). The laminated composites prepared from 0.05, 0.10 and 0.15 mm thick titanium foils are denoted later as samples Ti0.05 (12 layers of bronze and 11 layers of Ti), Ti0.10 (11 layers of bronze and 10 layers of Ti), and Ti0.15 (10 layers of bronze and 9 layers of Ti), respectively. After fabrication, the samples were cut using diamond blade and polished applying standard metallographic techniques.

Microstructural observations were performed using a JEOL JMS 5400 scanning electron microscope and a Nikon ECLIPSE MA 200 optical microscope. The chemical composition of the phases was determined by an energy dispersive spectroscopy utilizing a ISIS 300 Oxford Instruments.

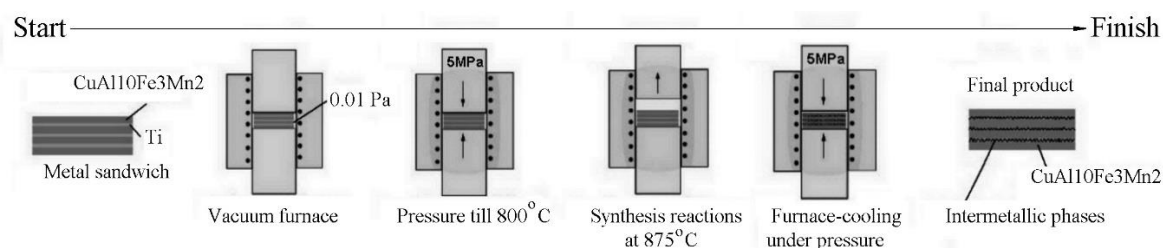


**Figure 1.** A schematic diagram of fabrication of CuAl10Fe3Mn2-intermetallic phases composite

Before the samples were examined with the optical microscope they had been etched to reveal grain boundaries and the structure of the intermetallic layers. Etching was performed with solution of 40 g CrO<sub>3</sub>, 7.5 g NH<sub>4</sub>Cl, 8 ml H<sub>2</sub>SO<sub>4</sub>, 50 ml HNO<sub>3</sub> and 1900 ml H<sub>2</sub>O. Vickers (HV0.1) measurements were performed by Matsuzawa microhardness tester. Samples with dimensions of 4 x 8 x 50 mm were subjected to tension test on an INSTRON screw machine at a constant crosshead speed of 0.1 mm/min. The Charpy impact tests were conducted on un-notched rectangular samples with dimensions of 4 x 4 x 40 mm on a pendulum impact tester with a maximum capacity of 24.5 J.

### 3 Results

After fabrication, the composition of synthesized phases in the composites was determined.

The previously published results [16] showed that only three intermetallic phases were formed in the processed samples: TiCuAl, TiCu<sub>2</sub>Al and Ti<sub>2</sub>Cu (figure 2). The predominant part of the intermetallic layers were TiCu<sub>2</sub>Al and TiCuAl phases, since a liquid front of reaction was moving into the aluminum bronze.

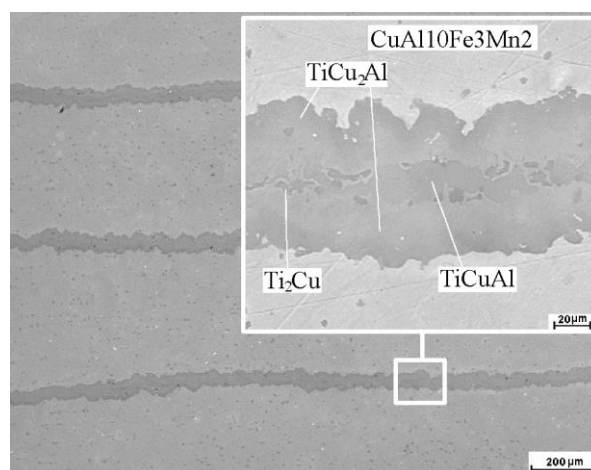


**Figure 2.** Microstructure of the CuAl10Fe3Mn2-intermetallic phases laminated composite

The laminated materials were well-bonded and nearly fully dense. The thickness of the intermetallic layers was dependent of the starting thickness ratio of the titanium and aluminum bronze foils. Microstructural investigations indicated also that the central zones of the formed intermetallic layers contained oxides inclusions which originated from surface oxide films on the used foils.

### 3.1 Microhardness measurements

Microhardness measurements were performed for used materials (for titanium grains and phases  $\alpha$  and  $\gamma'$  in aluminum bronze) as well as for formed intermetallic layers.

Results of microhardness measurements are given in table 2.

**Table 2.** Results of hardness measurements (HV0.1)

CuAl10Fe3Mn2	Titanium	Bronze/intermetallic interface	Middle of the intermetallic layer
222±97	215±5	715±55	530±20

The maximum hardness values in the range of 660 to 770 HV were achieved at the bronze/intermetallic interface due to the presence of the  $\text{TiCu}_2\text{Al}$  intermetallic phase. In the middle of the intermetallic layers, comprising mainly the mixture of  $\text{TiCuAl}$  and  $\text{Ti}_2\text{Cu}$  phases, hardness was a little bit lesser and contained in the range of 510 to 550 HV. In comparison, for materials used to produce the laminated composites, CuAl10Fe3Mn2 and titanium, the values of hardness were from two to four times lesser.

### 3.2 Tensile testing

Figure 3 shows the typical tensile stress-strain curves for the processed laminated composites and aluminum bronze.

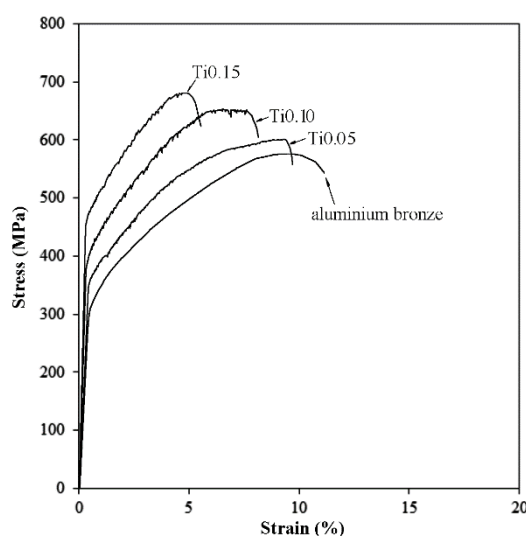


**Figure 3.** Tensile curves for the laminated composites and aluminum bronze

With an increase of thickness of the used titanium foils, the intermetallics layers grow, leading to an increase in the yield strength and the tensile strength of composites and a decrease in the total strain at fracture. The failure mechanism in the course of straining of the composites was carefully investigated. At the early stage of plastic straining the aluminum bronze grains were deformed by slip. No traces of plastic deformation were noticed in the intermetallic layers. Unfortunately, during deformation the crystal structures mismatch between phases makes almost impossible slip-bands slide through an alloy/intermetallic interfaces. Therefore, formation of cracks in the intermetallic layers was the characteristic feature of the prolonged deformation. The serrations in the stress-strain curves in figure 3 correspond to the formation of the multiple cracks in the intermetallic layers. The energy absorption capability of the aluminum bronze layers allowed numerous cracks to develop within each intermetallic layer before failure. With permanent increase of the crack number in the

intermetallic layers the bronze layers gradually underwent the total external load. As a result the plastic flow that took place in the alloy layers was restricted to the small regions between opposite cracks in the neighboring intermetallic layers. When the number and distribution of cracks reached a critical limit, the final failure occurred by shearing fracture of the aluminum bronze layers. Of course it is obvious that strain hardening of the tensile specimens (figure 3) was produced due to plastic deformation of the aluminum bronze layers. Table 3 summarizes the tensile properties of synthesized composites. The presented results the average of three measurements for each type of composite.

**Table 3.** Summary of tensile properties of CuAl10Fe3Mn2-intermetallics laminated composite

Sample designation	YS (MPa)	UTS (MPa)	Elongation (%)
<b>Ti0.05</b>	348±5	591±4	10±0.5
<b>Ti0.10</b>	377±4	656±2	8±0.4
<b>Ti0.15</b>	462±5	683±5	6±0.5

The obtained data are consistent with the results reported by Aleman et al. [3] and Vecchio et al. [5, 12, 17]. The authors demonstrated that fracture mechanism and failure energy in metal-intermetallic laminated composites were controlled by varying the intermetallic-to-metal volume ratio. The failure characteristic described for the aluminum bronze-intermetallic phases composites is strictly consistent with previous studies of cracking and damage mechanisms in various laminated composites [2-12, 17-22]. The damage mechanisms of the unlike laminated composites during tensile testing are alike because different intermetallics formed from different constituent metals behave very similar. They normally are brittle due to the limited mobility of dislocations, and have very low surface energy resulting in little or no plastic deformation at crack tips.

### 3.3 Impact test

For the impact toughness measurements, two loading directions were used: one in perpendicular and another parallel to the laminated composites.

Results of impact toughness measurements are listed in table 4 and they are the average of three measurements for each type of composite.

**Table 4.** The impact toughness of CuAl10Fe3Mn2-intermetallics laminated composite

Sample designation	Perpendicular to layers (J/cm <sup>2</sup> )	Parallel to layers (J/cm <sup>2</sup> )
<b>Ti0.05</b>	125±3	52±2
<b>Ti0.10</b>	117±4	44±3
<b>Ti0.15</b>	96±2	31±1

For the comparison also the impact toughness for aluminum bronze was measured and it was 67 J/cm<sup>2</sup>. Results shows that laminated composites exhibit anisotropic properties. When the load is applied perpendicular to the layers, the composites display superior impact toughness. Furthermore, it increases with increasing volume fraction of unreacted bronze. A crack initiated in the intermetallic layer did not travel across the specimen, but was arrested and deflected by the adjacent bronze layer. Further loading causes the formation of some new cracks in the next intermetallic layer. As a result a plastic strain of bronze was localized in shear bands between opposite cracks. This process was repeated until all the intermetallic layers have cracked resulting in tortuous crack propagation patch. Therefore there was one main crack and several branching smaller cracks. The failure occurred by cleavage mode showing extensive plastic deformation of bronze layers. It should be added that delamination or debonding of layers has been shown in the literature to be detrimental to the

performance of laminated composites [23, 24], but these failure mechanisms were not observed in any of tested samples. The absence of delamination of the bronze and intermetallic layers during mechanical testing is an indication of the excellent bonding between the layers. When the specimens were tested parallel to the layers the failure occurred by cleavage mode showing limited plastic deformation. It was evident that there was solely one main crack that travel across the specimen.

#### 4 Conclusions

The mechanical properties and fracture behavior of the CuAl10Fe3Mn2-intermetallic phases laminated composites have been examined under different loading conditions through tension and impact test.

The results of investigations indicated that tensile properties of the composites strongly depended on the proportion between thickness of individual bronze layers and the thickness of intermetallics. The yield and tensile strength of all investigated composites were higher than for aluminum bronze, and for Ti0.15 were higher even 40 and 18 %, respectively. The impact tests showed that when the load was applied perpendicular to the laminates, the composites displayed superior impact toughness, that was even 2 times higher than for bronze.

#### References

- [1] Wadsworth J and Lesuer D 2000 *Mater Charact* **45** 289
- [2] Shen Y L and Suresh S 1996 *Acta Mater* **44** 1337
- [3] Alman D, Dogan C P, Hawk J A and Rawers J C 1995 *Mat Sci Eng A-Struct* **192-193** 624
- [4] Bloyer D R, Venkateswara Rao K T and Ritchie R O 1997 *Mat Sci Eng A-Struct* **239-240** 393
- [5] Vecchio K S 2005 *JOM* **57** 25
- [6] Wang H, Han J, Du S and Northwood D O 2007 *Mat Sci Eng A-Struct* **445-446** 517
- [7] Konieczny M and Mola R 2008 *Steel Res Int* **79** 499
- [8] Konieczny M 2013 *Mat Sci Eng A-Struct* **586** 11
- [9] Konieczny M and Dziadon A 2007 *Arch Metall Mater* **52** 555
- [10] Dziadon A, Konieczny M, Gajewski M, Iwan M and Rzączyńska Z 2009 *Arch Metall Mater* **54** 455
- [11] Peng L M, Li H and Wang J H 2005 *Mat Sci Eng A-Struct* **406** 309
- [12] Harrach D J and Vecchio K S 2001 *Metall Mater Trans A* **32** 1493
- [13] Tixier-Boni S and Van Swygenhoven H 1999 *Thin Solid Films* **342** 188
- [14] Gazda A, Górny Z, Kluska-Nawarecka S, Saja K and Warmuzek M 2010 Effect of modification and heat treatment on structure and mechanical properties of CuAl10Fe3Mn2 bronze (Krakow: Works of Foundry Research Institute vol 12) p 37
- [15] Tsai H C, Higashi K and Sherby O D 1991 Proc. Int. Conf. of Advanced Composites (Warrendale: TMS) p 151
- [16] Konieczny M, Mola R, Kargul M and Aniołek I 2018 Proc. of 27th Int. Conf. on Metallurgy and Materials METAL (Brno) p 161
- [17] Rohatgi A, Harach D, Vecchio K S and Harvey K 2003 *Acta Mater* **51** 2933
- [18] Chung D, Kim J and Enoki M 2005 *Mater Sci Forum* **475-479** 1521
- [19] Xian L, Yanqing Y, Yungwang M, Bin H, Meini Y and Yan C 2007 *Scripta Mater* **56** 569
- [20] Buchholz F G, Rikards R and Wang A 1997 *Int Journal of Fracture* **86** 37
- [21] Rudnitskii N 2002 *Strength of Materials* **34** 612
- [22] Li M and Soboyejo 2000 *Metallurgical Trans A* **31** 1385
- [23] Li T, Grignon F, Benson D J, Vecchio K S, Olevsky E A, Schwarz R B and Meyers M A 2004 *Mat Sci Eng A-Struct* **374** 10
- [24] Odette G R, Chao B L, Sheckherd J W and Lucas G E 1992 *Acta Metall Mater* **40** 2381